

## Truncating *PICK1* Variant Identified in Azoospermia Affected Mitochondrial Dysfunction in Knockout Mice\*

Yao-qiang DU<sup>1, 2†</sup>, Chong-yi SHU<sup>3†</sup>, Min ZHENG<sup>3†</sup>, Wei-de XU<sup>2</sup>, Yue SUN<sup>2</sup>, Lu SHEN<sup>2</sup>, Chen ZHANG<sup>2</sup>, Yu-xin ZHANG<sup>2</sup>, Qian-ni WANG<sup>4</sup>, Kai-qiang LI<sup>1</sup>, Bing-yu CHEN<sup>1</sup>, Ke HAO<sup>1#</sup>, Jian-xin LYU<sup>2, 5#</sup>, Zhen WANG<sup>1, 2, 5#</sup>

<sup>1</sup>Laboratory Medicine Center, Department of Transfusion Medicine, Zhejiang Provincial People's Hospital, Affiliated People's Hospital, Hangzhou Medical College, Hangzhou 310014, China

<sup>2</sup>School of Laboratory Medicine and Life Sciences, Wenzhou Medical University, Wenzhou 325035, China

<sup>3</sup>Center for Reproductive Medicine, Department of Reproductive Endocrinology, Zhejiang Provincial People's Hospital, Affiliated People's Hospital, Hangzhou Medical College, Hangzhou 310014, China

<sup>4</sup>Department of Blood Transfusion, No.903 Hospital of PLA Joint Logistic Support Force, Hangzhou 310000, China

<sup>5</sup>School of Laboratory Medicine, Hangzhou Medical College, Hangzhou 310059, China

© Huazhong University of Science and Technology 2023

**[Abstract] Objective:** The protein interacting with C kinase 1 (*PICK1*) plays a critical role in vesicle trafficking, and its deficiency in sperm cells results in abnormal vesicle trafficking from Golgi to acrosome, which eventually disrupts acrosome formation and leads to male infertility. **Methods:** An azoospermia sample was filtered, and the laboratory detection and clinical phenotype indicated typical azoospermia in the patient. We sequenced all of the exons in the *PICK1* gene and found that there was a novel homozygous variant in the *PICK1* gene, c.364delA (p.Lys122SerfsX8), and this protein structure truncating variant seriously affected the biological function. Then we constructed a *PICK1* knockout mouse model using clustered regularly interspaced short palindromic repeat cutting technology (CRISPRc). **Results:** The sperm from *PICK1* knockout mice showed acrosome and nucleus abnormalities, as well as dysfunctional mitochondrial sheath formation. Both the total sperm and motility sperm counts were decreased in the *PICK1* knockout mice compared to wild-type mice. Moreover, the mitochondrial dysfunction was verified in the mice. These defects in the male *PICK1* knockout mice may have eventually led to complete infertility. **Conclusion:** The c.364delA novel variant in the *PICK1* gene associated with clinical infertility, and pathogenic variants in the *PICK1* may cause azoospermia or asthenospermia by impairing mitochondrial function in both mice and humans.

**Key words:** *PICK1*; azoospermia; truncating variant; knockout mice; mitochondrial dysfunction

Infertility is a global health problem that affects

Yao-qiang DU, E-mail: [duyaoqiang@hmc.edu.cn](mailto:duyaoqiang@hmc.edu.cn); Chong-yi SHU, E-mail: [shu\\_charming@163.com](mailto:shu_charming@163.com); Min ZHENG, E-mail: [zhengmin21@sina.com](mailto:zhengmin21@sina.com)

<sup>†</sup>The authors contributed equally to this work.

<sup>#</sup>Corresponding authors, Ke HAO, E-mail: [haoke@hmc.edu.cn](mailto:haoke@hmc.edu.cn); Jian-xin LYU, E-mail: [ljsx@hmc.edu.cn](mailto:ljsx@hmc.edu.cn); Zhen WANG, E-mail: [wangzhen@hmc.edu.cn](mailto:wangzhen@hmc.edu.cn)

\*This study was supported by grants from Zhejiang Provincial Natural Science Foundation of China (No. LQ21H200007), National Natural Science Foundation of China (No. 82202605, No. 81772664 and No. 82172363), Zhejiang Provincial People's Hospital Excellent Scientific Research Start-up Foundation of China (No. ZRY2019C008), and Hangzhou Medical College Fundamental Scientific Research Project of China (No. KYQN202116).

**Electronic supplementary material** The online version of this article (<https://doi.org/10.1007/s11596-023-2704-y>) contains supplementary material, which is available to authorized users.

more than 200 million couples worldwide, almost 10% of couples at reproduction age are infertile<sup>[1]</sup>. Approximately 20%–70% of infertility cases are attributed to male factors, which is called male infertility, and 30% of these are due to genetic defects in the male<sup>[2]</sup>. Infertility causes great mental stress and distress to couples of childbearing age<sup>[3]</sup>, leading to further aging of the population, which in turn creates a severe economic burden<sup>[4]</sup>. For male infertility patients with mildly impaired spermatogenesis, the chance of having offspring can be achieved by clinical methods of fertilization, including intracytoplasmic sperm injection (ICSI)<sup>[5, 6]</sup>. However, the genetic risks in male infertility and the immaturity of ICSI technology cannot be ignored. For example, in patients with no spermatogenesis (azoospermia), those with immature epididymal sperm, and those with very few sperm, there is currently no effective clinical treatment for infertility<sup>[7]</sup>. The pathogenic mechanism of azoospermia is complex, it often involves

abnormal energy metabolism of sperm, genetic risks, and abnormal signaling pathways in sperm. Little is known about the physiological pathology of spermatogenesis, its genetic causes, and genome consequences in gametes<sup>[8]</sup>. Therefore, azoospermia is a typical multifactorial disease with a strong genetic basis<sup>[9]</sup>. Approximately 30% of male patients indicated infertility due to chromosomal aberrations, Y chromosome microdeletions, single nucleotide variants and deletion variants<sup>[10]</sup>.

Various morphological abnormalities of the flagella (MMAF) phenotype also lead to male infertility<sup>[11]</sup>. A mouse model was constructed, showing that a variant in the *Tektin-t* gene can cause an abnormal morphological sperm function in male mice and significantly reduce sperm motility<sup>[12]</sup>. The *SEPT12* gene is downregulated in patients with azoospermia, and these patients discovered a few heterozygous variants in the *SEPT12* gene<sup>[13]</sup>. The deletion of the *Slc26a8* gene in mice lead to complete lost of sperm motility and flagella in the tail of the sperm<sup>[14]</sup>. It has been shown that the loss of calmodulin- and radial-spoke-associated complex protein CFAP251 can cause infertility<sup>[15]</sup>. The protein interacting with C kinase 1 (*PICK1*) gene has been mainly studied in the field of nervous system and cancer research since its discovery in 1995<sup>[16]</sup>. A study of *PICK1* knockout mice showed their clinical symptoms were very similar to those of human round spermatozoa<sup>[17]</sup>. The study of testicular sections suggested that deleterious variants in this gene caused defects in spermatogenesis. The laboratory speculated that after the *PICK1* gene was knocked out, acrosome fragmentation occurred in the early stages of sperm formation. This was immediately followed by deformation and defects in the formation of mitochondrial sheaths, which eventually led to clinical manifestations from which several variants have been found, such as a homozygous missense *PICK1* variant in a Chinese family, which can cause round head deformities of the sperm, decreased sperm density, and severe damage to sperm motility<sup>[18]</sup>. More than 60% of normal semen is secreted by the seminal vesicles, 20% to 30% comes from the prostate, approximately 10% comes from the epididymal fluid and sperm, and a small amount is secreted by the urethral glands. The classic hemostatic system similar to blood in the semen and high molecular weight seminal vesicle (HMW-SV) protein system coexist, and these two work together to regulate semen coagulation and liquefaction<sup>[19,20]</sup>. These may cause coagulopathy in patients with reproductive disorders.

*PICK1* is a multifunctional binding protein that is widely distributed in various cells of the nervous system<sup>[21]</sup>. It is closely related to central nervous system disease, pain, insulin secretion, tumorigenesis, and tumor development, and also participates in membrane

receptor transport<sup>[17]</sup>. The *PICK1* protein contains BAR and PDZ domains, which can bind to the C-terminus of the phospholipid bilayer and various transmembrane receptors to regulate the expression and endocytosis on the cell membrane of these receptors<sup>[22]</sup>. *PICK1* is expressed not only in the brain but also in many other tissues. It shows relatively high levels of expression in the testes and pancreas<sup>[23]</sup>. It is known that male *PICK1* knockout mice are completely sterile<sup>[17]</sup>. Round-headed spermatozoa in *PICK1* knockout mice have deformed neurons and abnormally shaped nuclei, and *PICK1* is localized to Golgi-derived acrosomal particles in sperm<sup>[24]</sup>, maybe the round-headed spermatozoa phenotype of *PICK1* knockout mice is the result of abnormal acrosomal particles leading to impaired acrosome formation. Multiple morphological abnormalities of the acrosome and mitochondrial phenotypes are one of the most severe forms of sperm defects causing male infertility<sup>[25, 26]</sup>. This unique phenotype is characterized by the presence of immobile sperm upon ejaculation, and it exhibits several serious sperm abnormalities, including abnormal sperm structure and impaired sperm motility.

## 1 MATERIALS AND METHODS

### 1.1 Human Clinical Sample

We collected samples from azoospermia infertile patients in the Department of Reproductive Endocrinology in our hospital. The Research Ethics Committee of Zhejiang Provincial People's Hospital approved of the collection of samples for research (No. 2021QT431), and informed consent was obtained from each patient. According to the WHO textbook, "Human Semen and Sperm-Cervical Mucus Interaction Laboratory Manual, 4th edition," participants were abstinent for 3–7 days and semen was collected by masturbation. The selection criteria included couples living together for more than one year after marriage with a normal sex life and engaged in no contraceptive measures. Sufficient semen was obtained, and routine analysis of semen was performed more than two times. Inclusion criteria of the subjects were as follows: absence of drug or alcohol intake on the day of semen examination, a semen volume 1.5–6 mL, gray or pale yellow, all liquefaction within 1 h; total sperm motility, total sperm count, progressive movement (PR) + non-progressive movement (NP), and forward sperm motility rate was 0. Additionally, the specimens were divided into different grades according to the forward sperm activity rate: mildly weak sperm,  $20 \leq PR < 32$ ; moderately weak sperm,  $10 \leq PR < 20$ ; and severely weak sperm,  $0 \leq PR < 10$ . The sperm morphology was observed; seminal plasma anti-sperm antibody was detected; blood and urine routine examination, liver and kidney function detection were performed.

## 1.2 Semen Analysis and Sperm Morphological Study

After 2–7 days of abstinence, semen samples from human subjects were collected by masturbation and examined after liquefaction at 37°C for 30 min. Assessments of the semen volume, sperm concentration, and viability were performed according to WHO guidelines. Semen analysis was repeated at least twice. A semen sample from a mouse model was collected from the epididymis, diluted in 1 mL of sperm rinse (Vitrolife, Sweden), and examined after being incubated at 37°C for 30 min.

## 1.3 Sanger Sequencing and Protein Structural Modeling

Genomic DNA was extracted from whole blood samples taken from the patient using a Quick DNA Extraction Kit (Takara, Japan). Subsequently, 2.5 ng/μL genomic DNA (gDNA) (10-μL reactions) was amplified using 35 cycles of PCR on a C1000 thermal cycler (Bio-Rad, USA) with 2× Flash Hot Start Master Mix (dye) (Takara, Japan) and 20 pmol of gene-specific primers<sup>[27]</sup>. The primer sequences used to amplify *PICK1* exons are found in table S1. PCR products were purified with a DNA clean-up kit (CW2301, CWBIO). Using a 3730xl genetic analyzer, the purified amplicons were directly cycle sequenced in both directions with a BigDye Terminator v3.1 cycle sequencing kit (Applied Biosystems, USA) containing *PICK1* forward or reverse sequencing primers and then precipitated using ethanol and detected via capillary electrophoresis using Sequence Analysis 6.0 software (Applied Biosystems, USA) and Chromas 2.23 software (Technelysium, Australia). Exon sequencing was performed, as previously described for individual samples<sup>[27]</sup>. Sequencing reactions were carried out using a BigDye Terminator v3.1 cycle sequencing kit (Applied Biosystem, USA).

The tertiary structures of human wild-type and mutant *PICK1* were predicted using Robetta software (<https://rosetta.bakerlab.org/software>), and the results were saved as a PDB file. We used PyMOL (<http://pymol.org/>) to visualize the structures of these proteins.

## 1.4 Animal Model

For all of the experiments involving mice, animals were processed and euthanized according to methods approved by the Animal Protection and Use Committee of Zhejiang Provincial People's Hospital. All mice used in the study were male adult (8–9 weeks) mice. Two groups of male C57/BL6 mice were studied separately: wild-type (*PICK1* +/+), *PICK1* heterozygous (*PICK1* +/-), and *PICK1* knockout (*PICK1* -/-) mice. *PICK1* gene knockout C57/BL6 mice were obtained in the reproductive stage from Zhejiang University Laboratory Animal Center. During the breeding process, *PICK1* +/- (♂) and *PICK1* +/- (♀) mice were crossbred to obtain

*PICK1* -/- (♂) combined experimental mice<sup>[17]</sup>. After the male mouse was sacrificed, the testes, epididymis, and vas deferens were aseptically separated and rinsed in a petri dish. The epididymal head was discarded, and the epididymal tail was left, which was cut into several sections and opened with surgical scissors to allow the sperm to float in the culture. Totally, 10 μL of sperm were placed on a special sperm counting board, and the total number of sperm in 100 grids were counted<sup>[28]</sup>.

## 1.5 PCR Identification of *PICK1* Knockout Mice

According to the instructions provided by the manufacturer, we removed the toes of mice, added 20 μL of Additive 1 (AD1) buffer and 5 μL of Additive 2 (AD2) buffer in the TranDirect Animal Tissue PCR kit, mixed by pipetting, and incubated at room temperature for 10 min, then incubated at 95°C for 3 min. Finally, we added 20 μL of Additive 3 (AD3) buffer. The PCR reaction system was as follows: 0.5 μL 10 μmol/L primer *PICK1*-1, 0.5 μL 10 μmol/L primer *PICK1*-2, 0.5 μL 10 μmol/L primer *PICK1*-3, 10 μL Taq mix (2×), 2 μL template were sequentially added, and water was added to reach 20 μL. The PCR reaction conditions were: denaturation at 95°C for 30 s, annealing at 62°C for 30 s, extension at 72°C for 30 s, and the cycle continued 35 times. The primer sequences were as follows: *PICK1*-1, 5'-TCACTTGCCAGAGGAGAAAAGT-3'; *PICK1*-2, 5'-AAAAATAGGCGTATCACGAGGC-3'; *PICK1*-3, 5'-CACTCGCAGCTTGTCTGATCTG-3'.

## 1.6 Western Blotting of *PICK1* Knockout Mice

Briefly, an equivalent amount of protein from each sample was separated by 10% SDS-PAGE and transferred to PVDF membranes (Millipore, Billerica, MA). The membranes were then blocked in 5% milk for 1 h at room temperature and then incubated with respective primary antibody overnight at 4°C including anti-*PICK1* (Neuromab, Davis City, CA, USA) and anti-GAPDH (Huaan, China). Membranes were then incubated with HRP-conjugated secondary antibody (Huaan, China). After washing, protein bands were visualized using ECL reagents (Beyotime, China) and captured by Bio-Rad image system (Bio-Rad, California, USA). Protein bands were analyzed by Image J software, and results were normalized to the respective GAPDH bands.

## 1.7 Detection of Sperm Adenosine 5'-Triphosphate (ATP) Level

The ATP assay kit was manufactured by Beyotime, and the assay was performed according to the manufacturer's instructions. It is used to detect ATP levels in common solutions, cells, or tissues. We used an ATP enhancement kit where ATP provides energy when luciferin produces fluorescence based on firefly luciferase (also known as luciferase). A 50-μL aliquot of the diluted sperm suspension was added to 100 μL of cell lysis reagent and incubated for 5 min at room temperature. The resultant cell lysate was recovered

for the supernatant. Bioluminescence of the samples was measured in triplicate in a 96-well plate using a luminometer. Following the manufacturer's protocol, 50  $\mu\text{L}$  of luciferase working reagent was added to 20  $\mu\text{L}$  of sample in each well, and light emission from the resulting reaction was measured. The dilution ratio of the ATP solution to the cell lysis reagent was used to calculate the ratio of ATP in the sample.

### 1.8 Measurement of Sperm Reactive Oxygen Species (ROS)

Sperm mitochondrial generation of ROS was determined by chemiluminescence measurement. Briefly, 100  $\mu\text{L}$  of washed sperm suspension at a concentration of  $5 \times 10^6$  sperm/mL was placed in an EP tube. Then, freshly prepared probe 2',7'-dichlorodihydrofluorescein diacetate (DCFH-DA) (Beyotime, China) was dissolved in phosphate-buffered saline (PBS) (10  $\mu\text{mol/L}$  final concentration) and 100  $\mu\text{L}$  was added to each sample. Briefly, sperm were stained with DCFH-DA working staining solution, incubated for 15–20 min. Spermatozoa in the unbound portion were washed with PBS and centrifuged for 5 min at  $600 \times g$  at  $4^\circ\text{C}$ . Fluorescence luminescence mode was selected and used to detect ROS using a multifunction microplate reader. The remaining part of the sperm was applied to a glass slide, and an anti-fluorescent quencher containing 4', 6-diamidino-2-phenylindole (DAPI) was added to the smear. The smear was observed under a fluorescence microscope before the cover glass was coated.

### 1.9 Sperm Mitochondrial Membrane Potential (MMP) Assessment

Florescent probes of 5, 5', 6, 6'-tetrachloro-1, 1', 3, 3'-tetraethylbenzimidazolyl-carbocyanine iodide (JC-1) (Beyotime, China) were used in the assessment of the sperm MMP of different sperm samples<sup>[29]</sup>. Briefly, sperm samples were stained with a working solution of JC-1 stain (5  $\mu\text{g/mL}$ ) and incubated for 15–20 min. The spermatozoa in the unbound portion were washed with JC-1 buffer (1 $\times$ ) and centrifuged for 5 min at  $600 \times g$  at  $4^\circ\text{C}$ . The pellet obtained was smeared over a glass slide, and anti-fluorescence quencher containing DAPI was added to the smear before a cover slip was applied to the slide. The slide was then observed under a fluorescent microscope using the procedure described below. The slide with the sample was mounted onto a clean glass slide along with a cover slip and examined using a fluorescent microscope (Nikon ECLIPSE Ti-s, Japan) using a fluorescein-isothiocyanate (FITC) filter (emission: 515–555 nm; excitation: 465–495 nm) and a tetramethylrhodamine-isothiocyanate (TRITC) filter (emission: 554–576 nm; excitation: 540 nm). The images from the two filters were merged into a final image. The spermatozoa with a high MMP were yellow-red, whereas the spermatozoa with a low MMP were fluorescent green.

### 1.10 Statistical and Bioinformatics Analyses

Measurement data were expressed as mean $\pm$ SD, and an independent samples *t*-test was used to compare data between multiple groups using Graphpad Prism 6.0. A value of  $P < 0.05$  indicated that the difference was statistically significant. BLAST (<https://blast.ncbi.nlm.nih.gov/Blast.cgi>) and BioEdit (version 7.0.5.3) were used for simultaneous sequence comparison with database and sequence visualization. The variant was annotated by ANNOVAR (<http://annovar.openbioinformatics.org/en/latest/>) and an in-house bioinformatics tool with the UCSC annotation (based on GRCh37, hg19). We obtained the minor allele frequency (MAF) according to normal population variant databases, including the dbSNP150 (<http://www.ncbi.nlm.nih.gov/projects/SNP/>), 1000 Genomes Project (<http://www.1000genomes.org/>), ESP6500 (<http://evs.gs.washington.edu/EVS/>), and ExAC (<http://exac.broadinstitute.org/>) databases.

## 2 RESULTS

### 2.1 Clinical Data and Specimen Information

In this study, we detected several patients, and screened out one significant sample. This patient was 28 years old (when the sample was collected) and cohabited with his partner for more than one year without using contraception and fertility measures. A clinical diagnosis was obtained in our hospital after two years of marriage without contraception or fertility for the patient. Conventional computer-aided analysis of semen volume was 3.0 mL and the sperm concentration was 0.0 million/mL. The total amount of seminal plasma neutral alpha-glucosidase was 0.6 U/L at ejaculation, and the total amount of refined berry sugar was 0.6 mmol/L at ejaculation. Physical examination showed a normal testis size on both sides, swelling and tenderness of the right epididymis, and unsatisfactory palpation of the vas deferens. Therefore, this indicated malformation of the vas deferens, epididymis, seminal vesicles and prostate led to the diagnosis of azoospermia (table 1).

A biopsy of the right testis showed a very finely curved seminiferous tubule-like tissue, which is fragile to touch. This was sent for pathological examination. An ultrasound promptly showed an absence of the left seminal vesicle glands and a cystic structure in the right seminal vesicle gland area (fig. 1A, fig. S1A), as well as an absent bilateral vas deferens, left epididymal tail dysplasia, bilateral epididymal stasis, bilateral varicocele, and left testicular sheath cavity stones (fig. 1B, fig. S1B). A small amount of sample was submitted for a testicular biopsy, including the spermatogenic tubules, thickened basement membranes. The significantly reduced spermatogonia were observed, and no clear mature sperm was found in the cavity



**Table 1 Information of basic clinical and laboratory analysis**

Clinical indicator	Result	Standard value	Qualitative
Total seminal $\alpha$ -glucosidase (U/L seminal fluid)	0.6	$\geq 10.12$	↓
Total refined sugar (mmol/L seminal fluid)	0.6	$> 8.33$	↓
Dilution ratio	Undiluted		
Abstinence days	4	2–7 days	
Semen volume (mL)	3.0	$\geq 1.5$	
Semen color	Gray	Gray	
Semen smell	normal		
pH	7.50	7.2–8.0	
Viscosity (cm)	$>2$	$< 2$	↑
Semen liquefaction time (min)	$<30$	$< 60$	
Sperm concentration (million/mL)	0.0	$\geq 15$	↓
Sperm count (million)	0.0	$\geq 39$	↓
Total forward sperm (PR) (million)	0.0		
Round cell (cells/HP)	0–2		

PR: progressive movement

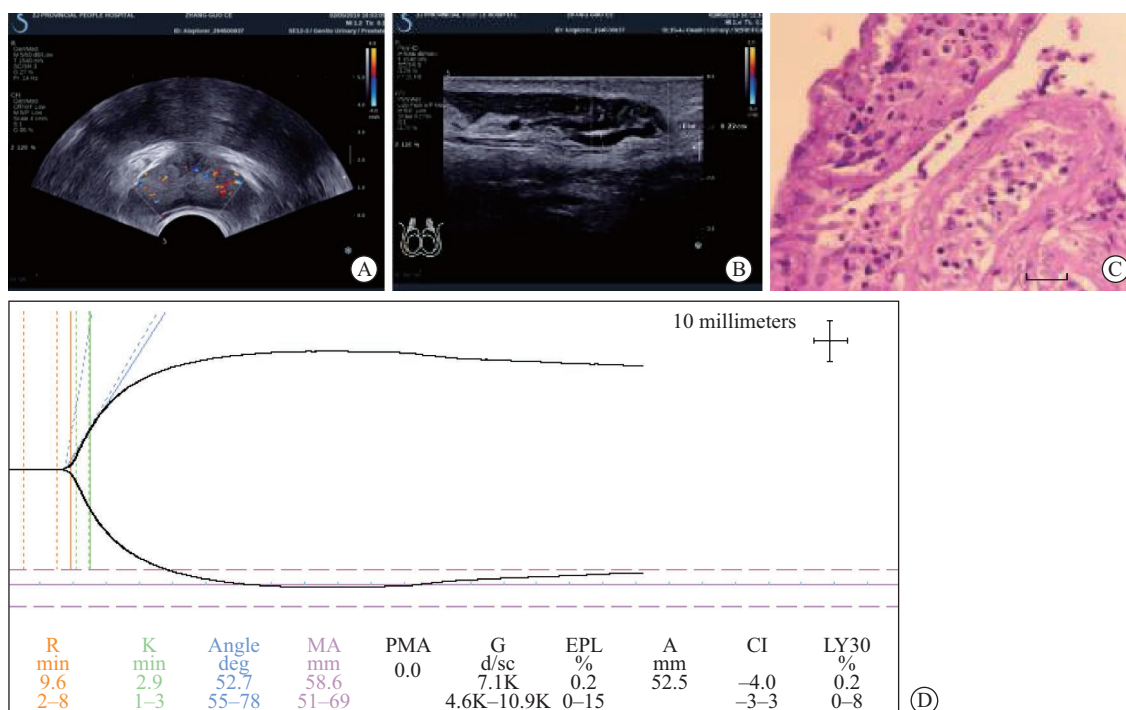


**Fig. 1** Clinical pathology results of a representative patient

A: the abdominal ultrasound image of transrectal prostate and seminal vesicles; B: the superficial ultrasound image of testis, epididymis and spermatic cord; C: pathological diagnosis of puncture testicular mass (magnification  $\times 200$ , scale bar= $5 \mu\text{m}$ ); D: thromboelastography result

(fig. 1C). Furthermore, the thromboelastography values of the R (min) and Angle ( $\alpha$ ) indicated that the coagulation function of coagulation factors and fibrin were reduced (fig. 1D, table S2). It is possible that the change of coagulation functions could affect the male reproductive function<sup>[30]</sup>.

### 2.2 Identification of the Novel Variant

Here, we sequenced all the exon regions of *PICK1* from the patient, and found a harmful homozygous variant in the gene, the c.364delA (p.Lys122SerfsX8) (fig. 2A, table S3). We also found that this variant was not presented in large public control populations, including studies from the dbSNP150, 1000 Genomes, ESP6500, and ExAC databases. Similarly, according

to a search of the published literature, this variant has not been previously reported. The mutant amino acid is highly conserved in different species homologous to humans (fig. 2B), which leads to a frameshift variant in the coding portion of the exon 6 protein, and the amino acid of the eighth shift code is thus terminated early (fig. 2C). The AH domains of the protein have important functions, and this termination of protein coding leads to the protein not being able to be translated (fig. 2D).

### 2.3 Protein Structural Modeling of the Variant

The *PICK1* protein (<http://www.uniprot.org/uniprot/Q9NRD5>, ENSG00000100151) consists of an N-terminal PDZ domain and C-terminal AH domain (fig. 2D). The PDZ domain is located between amino acids

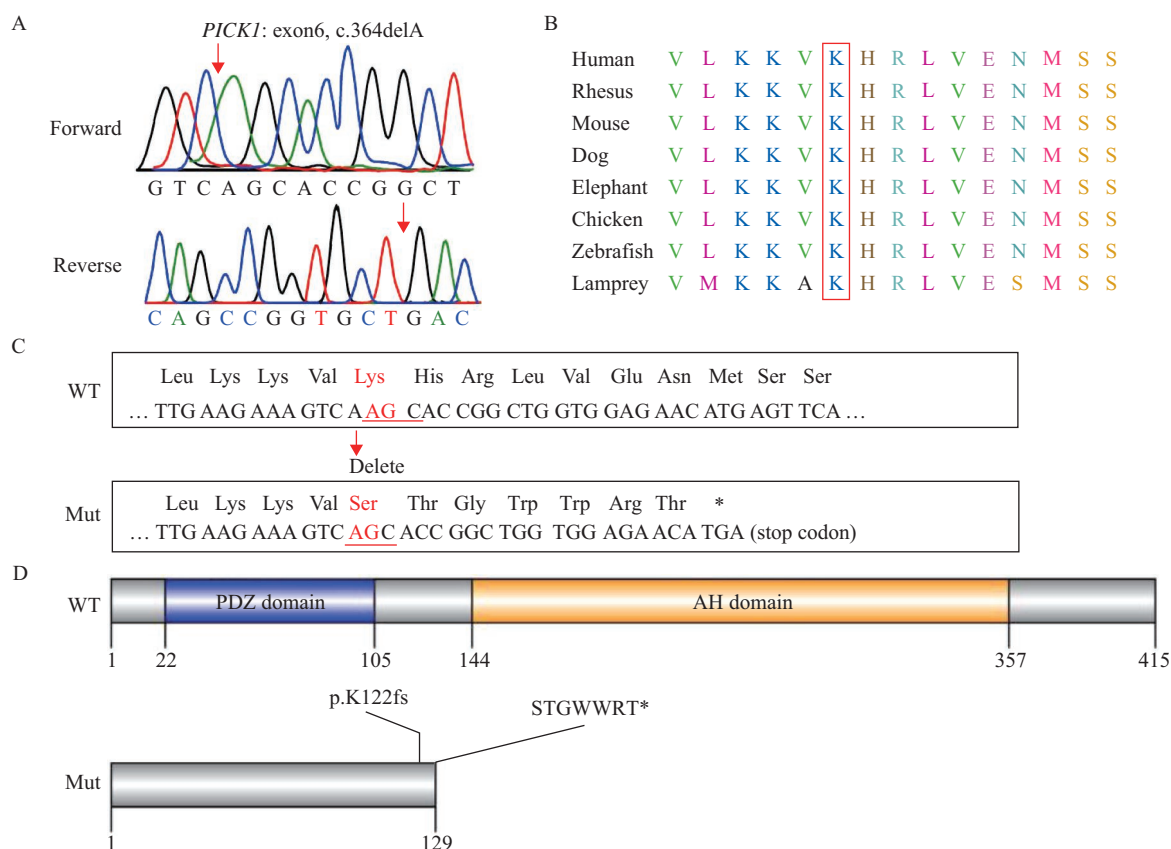


**Fig. 2** A homozygous variant was identified in *PICK1*

A: sanger sequencing in the forward and reverse; B: conservation of the variant c.364delA (p.Lys122SerfsX8) among different species; C: nucleotide sequence of deletion in exon 6; D: protein schematic of *PICK1*. WT: wild-type, Mut: mutant-type, \*: premature stop codon

22–105, with the remaining part of *PICK1* comprising the C-terminal AH domain (144–357). Using Robetta software, we predicted the 3D structure of the wild-type *PICK1* protein (1–415) and mapped out the Ser122 residue in the structure (fig. 3A). The p.Lys122SerfsX8 variant results in a protein product with a deletion of the entire C-terminal AH domain (fig. 3B). The truncating variant at this key region may lead to protein dysfunction and therefore contribute to disease pathogenesis.

#### 2.4 Comparison of the Phenotype of *PICK1* Wild-type and Knockout Mice

During the breeding process, *PICK1*  $+/-$  ( $\sigma$ ) and *PICK1*  $+/-$  ( $\phi$ ) mice were crossbred to obtain *PICK1*  $-/-$  ( $\sigma$ ) combined experimental mice, as identified by PCR and Western blotting (fig. S2). The basic characteristic differences between the wild-type and knockout mice were obtained. We found that the *PICK1* knockout mice showed no fertility, the ratio of testis to body weight was significantly reduced, semen routinely showed a significant decrease in the total number of sperm, and testicular slices showed a significant decrease in various types of spermatogenic cells (table S4). Moreover, we extracted the testicular tissue in wild-type and knockout mice, and compared these under a microscope at 20 $\times$  and 40 $\times$  fields of view (fig. 4A). The immunohistochemical results indicated

that the sperm counts were significantly decreased [wild-type vs. knockout,  $(46.33 \pm 6.96) \times 10^6$  vs.  $(6.33 \pm 0.88) \times 10^6$ ,  $P < 0.001$ ] and that the sperm showed a partial deformity (fig. 4B).

#### 2.5 ATP Levels not Changed in *PICK1* Knockout Mice

To further explore whether there were differences in the function of sperm mitochondria between the wild-type and knockout mice, we performed mitochondrial function tests for the mice of each group. We analyzed the ATP levels of each group and found no significant differences between the groups (fig. 5A). The mitochondrial ATP levels between the knockout and wild-type mice were not significantly different ( $P > 0.05$ ). The motility of sperm requires mitochondria to produce ATP to provide energy, while sperm motility is the main physiological determinant of male fertility.

#### 2.6 ROS and MMP Levels Significantly Changed in *PICK1* Knockout Mice

For the qualitative and quantitative analyses of the levels of ROS in each group (fig. 5B), we found that the spermatozoa levels of the knockout mice were significantly higher than those of the wild-type mice ( $P < 0.001$ ). The generation of ROS is an early event in a series of modifications that occur during sperm capacitation. However, changes in cellular redox

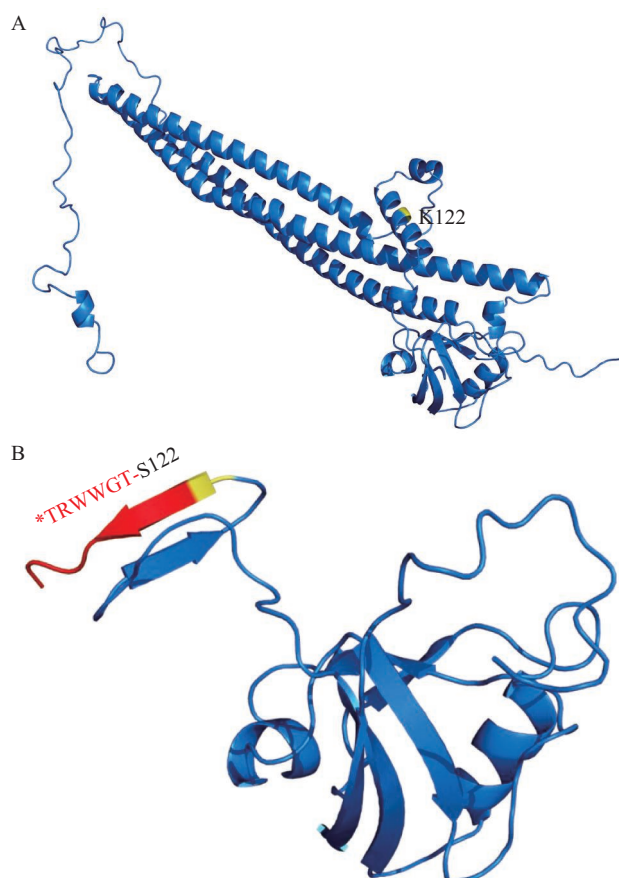


**Fig. 3** Structural difference between wild-type and truncating PICK1 protein

A: function prediction of the wild-type (full-length) PICK1 protein; B: truncating protein (p.Lys122SerfsX8) is represented, with the variant site shown in yellow, and the range of red fragments representing the frameshift allele amino sequence (-TRWWRT\*).

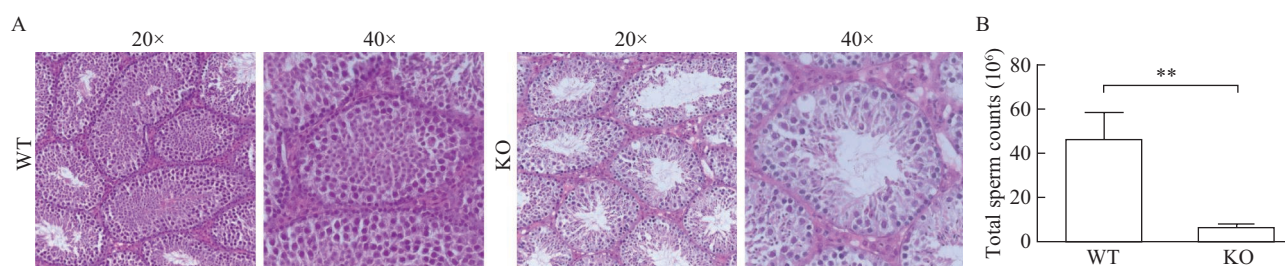


**Fig. 4** Immunohistochemical results in WT and KO mice testis

A: immunohistochemical images in the 20× and 40× fields of view; B: comparison of total sperm counts from bilateral epididymis, WT vs. KO:  $(46.33 \pm 6.96) \times 10^6$  vs.  $(6.33 \pm 0.88) \times 10^6$ , mean ± SEM,  $n=3$ . WT: wild-type; KO: knockout; \*\* $P < 0.001$

of *PICK1* from an infertile male azoospermia patient and found a harmful frameshift variant c.364delA (p.Lys122SerfsX8), which led to the premature termination of protein coding. *PICK1* is an evolutionarily conserved protein that shows high-level expression in the testis<sup>[17]</sup>. The sperm structural analysis in the knockout mice showed that the mitochondrial ridge disappeared after the knockout of *PICK1*. However, histological analysis of the testes of these mice showed that all the spermatogenic stages of the spermatogenic epithelium were present, suggesting that the overall process of spermatogenesis was preserved

homeostasis lead to sperm senescence and eventually, cell death. ROS cause oxidative cell damage and inhibit sperm function. We found that the sperm fluorescent intensity revealed that the knockout mice have significantly higher sperm ROS levels than wild-type mice (fig. 5B). Furthermore, after *PICK1* knockout, the sperm mitochondria were abnormally located and transferred from the middle of the sperm to the head of the sperm (fig. 5C). Through the detection of sperm ROS, the knockout mice showed a significant increase in ROS and a significant decrease in mitochondrial function compared to wild-type mice.

By comparing the membrane potential levels between the groups, the JC-1 fluorescent probe staining results showed that the red fluorescence in wild-type mice sperm was stronger than the green fluorescence (fig. 6A). We also found that the membrane potential level of wild-type mice sperm was significantly higher than that of knockout mice ( $P < 0.001$ ) (fig. 6B). When the MMP is high, JC-1 accumulates in the matrix of the mitochondria to form a polymer that produces red fluorescence. When the MMP is low, JC-1 cannot aggregate in the matrix and only monomers can be formed, resulting in green fluorescence. After *PICK1* knockout was performed, the mouse sperm mitochondria became abnormally located and the MMP decreased, which led to a decrease in mitochondrial function.

### 3 DISCUSSION

In this study, we sequenced all the exon regions

but the mature sperm might be defective.

Male infertility remains a persistent problem, the occurrence of weak spermatozoa is affected by genetic and environmental factors, and the causes of the disease are often complicated and involve many clinical genetic risk factors<sup>[31]</sup>. Considerable efforts have been made to identify and characterize the several numbers of genes involved in sperm from individuals with male infertility, including key genes such as *CFTR*, *BPY2*, *CDY*, *DAZ*, *HSFY*, *PICK1*, etc<sup>[9, 32]</sup>. *PICK1* variants in azoospermia may be associated with an abnormal functioning of the testicular epididymis or other related

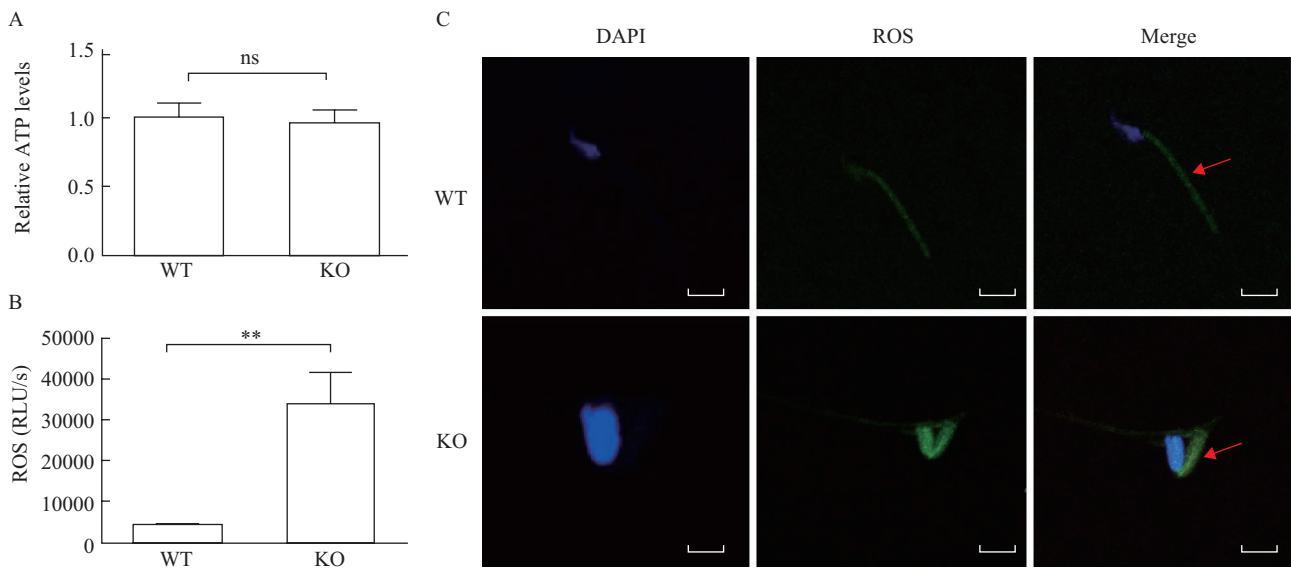


**Fig. 5** Detection of sperm ATP and ROS levels in different mice

A: no significant difference in ATP levels between WT and KO mice; B: sperm fluorescence intensity; C: sperm DCFH-DA fluorescence staining (indicated by arrows). Scale bar=10  $\mu$ m; Green indicates staining of mitochondrial ROS probe; blue indicates nuclear staining. WT: wild-type; KO: knockout; ns: not significant; \*\* $P$ <0.001

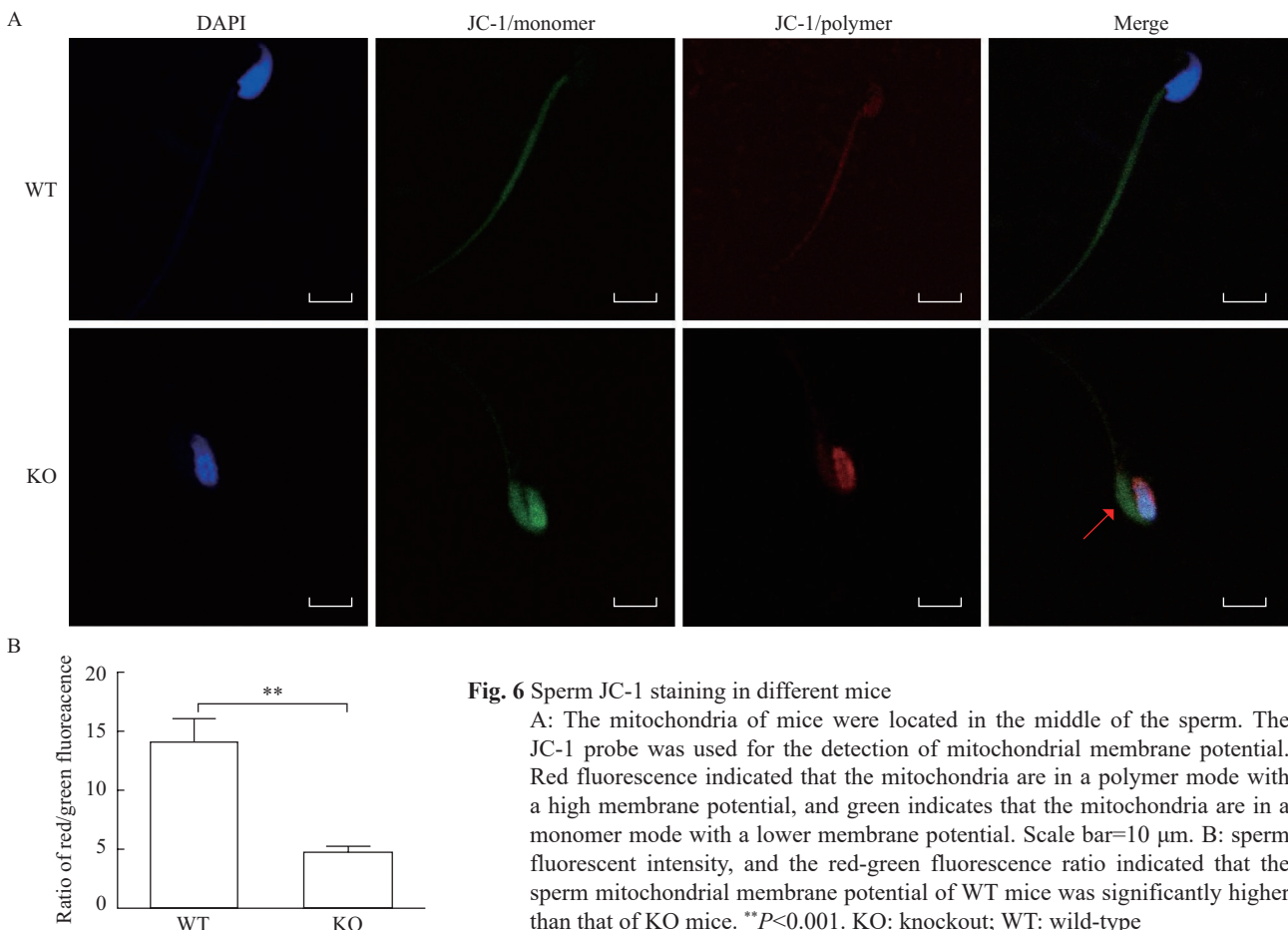


**Fig. 6** Sperm JC-1 staining in different mice

A: The mitochondria of mice were located in the middle of the sperm. The JC-1 probe was used for the detection of mitochondrial membrane potential. Red fluorescence indicated that the mitochondria are in a polymer mode with a high membrane potential, and green indicates that the mitochondria are in a monomer mode with a lower membrane potential. Scale bar=10  $\mu$ m. B: sperm fluorescent intensity, and the red-green fluorescence ratio indicated that the sperm mitochondrial membrane potential of WT mice was significantly higher than that of KO mice. \*\* $P$ <0.001. KO: knockout; WT: wild-type

organs. The expression levels of *PICK1* in different organs in the GTEx dataset showed that the *PICK1* protein was significantly expressed in the testes and prostate tissues (fig. S3). The probability and causes of *PICK1* variants in the population were not frequently found, such as G393R and G198A<sup>[18, 32]</sup>, and the clinical

significance of these variants usually manifested as a reduced sperm count (oligozoospermia), a reduction in sperm motility (weak spermatozoa), a higher proportion of abnormal sperm in ejaculation (abnormal spermatozoa), or a combination of these defects. The advent of exon sequencing technology has facilitated



the identification of potentially responsible genetic variants in infertile men, but detailed studies of the functions of these genes in spermatogenesis of humans are often not available, thus the development of animal models is required. Moreover, many mutant mouse models with spermatogenesis defects have been identified, and molecular and genetic studies of spermatogenesis in these models have led to a deeper understanding of spermatogenesis.

We collected blood samples from patients to conduct full exon sequencing of the *PICK1* gene, as 85% of the variants that cause disease are reported to be in the coding and functional regions of the gene. Exon sequencing reveals the occurrence of genetic disease variants. After searching for variants and verifying by Sanger sequencing in the BLAST dataset, we found that compared to normal gene sequences, there were multiple variants in the *PICK1* gene in patients with azoospermia, most of which are single nucleotide variants (SNVs). Therefore, we speculate that the *PICK1* gene is involved in the occurrence and development of azoospermia, and its variants are part of the gene weakening of sperm motility, by integrating the genetic model and molecular dynamic simulation methods in our recent study<sup>[33, 34]</sup>.

Many studies often use knockout mice to analyze the clinical effect of genetic truncating variants<sup>[23, 32]</sup>. Multiple methods were used to suppress the expression of genes in mice, and explore the function mechanism of this gene<sup>[35]</sup>. Some studies in the literature indicate that a lack of *PICK1* in mice can cause male infertility due to reduced sperm counts and severely impaired sperm motility. The main defects of sperm are acrosome deformity, an abnormal arrangement of a round nucleus, and an abnormal mitochondrial sheath, which are also prominent features of the global sperm disease<sup>[36]</sup>. The main function of mitochondria is to synthesize ATP through oxidative phosphorylation and provide energy for various activities of cells. ATP and adenosine triphosphatase (ATPase) play an important role in the movement of sperm. They are involved in the energy response and motility of sperm. Just as ATP provides large amounts of energy when muscle fibers contract, ATP provides the energy required for sperm fiber contraction. In our study, it is shown that after *PICK1* is knocked out, not only is the mitochondria localized abnormally in the sperm, but metabolic functions are also changed. It has been confirmed that mitochondria contain enzymes involved in oxidative phosphorylation energy metabolism, which plays a key role in cellular energy metabolism. The mitochondrial sheath in the middle piece provides the energy required for sperm movement. Many factors that affect ATP production can directly or indirectly affect sperm motility. Recently, the correlation between an abnormal mitochondrial

structure, function and low sperm motility has attracted much attention. The sperm mitochondria of the *PICK1* knockout mice were transferred from the original tail arrangement to the head, resulting in a lack of sperm tail movement energy and weakened vitality.

In the process of oxidative respiration, mitochondria store the generated energy in their inner membrane in the form of electrochemical potential energy, causing an asymmetric distribution of protons and other ions on both sides of the inner membrane to form MMP. MMP is a metric that reflects the energy status of the mitochondria, and it is the earliest factor in the initiation of the process of apoptosis. A normal level of MMP is a necessary condition of maintaining normal functioning of the mitochondria<sup>[37]</sup>. The sperm MMP decreases, and the ability to scavenge active oxygen weakens, leading to the accumulation of active oxygen in the sperm, and the overall quality of sperm decreases. A small amount of ROS has a positive effect on sperm. For example, sperm capacitation and acrosome reactions require a small amount of ROS. Excessive amounts of ROS not only affect sperm morphology and motility (such as abnormal sperm tail mitochondria, mainly caused by lipid peroxidation of organelle membranes), but the most important thing is the destruction of sperm DNA, which occurs when ROS directly attack the organs<sup>[38]</sup>. And the large molecules directly removed the purines or bases, which leads to the lack of formation of purine or apyrimidinic sites in nucleic acids. Another important note is that ROS directly attack the structures of superoxide dismutase and glutathione peroxidase (GSH-Px), thereby affecting DNA repair mechanisms<sup>[39]</sup>. Sperm activity consumes a high amount of energy, and the lack of this energy will inevitably lead to the decline of sperm motility. Mitochondria are factories that produce energy in humans, and they play a vital role in propagating sperm activity. Studies have also found that patients with weak spermatozoa have more mitochondrial dysfunction and gene variants than normal sperm<sup>[40, 41]</sup>. Variants in mitochondrial genes may be induced by sperm isolation and morphological changes of sperm. The key finding of our study is the isolation of the novel variant in the *PICK1* gene as sequenced by exon sequencing, which is associated with clinical infertility. Pathogenic variants in the *PICK1* gene may cause azoospermia or asthenospermia by impairing mitochondrial function in both mice and humans. With the in-depth study of mitochondrial DNA, there have been an increasing number of studies on azoospermia and mitochondrial genes, but more experiments are still needed to reveal the underlying relationship.

#### Conflict of Interest Statement

The authors have no conflicts of interest.

## REFERENCES

- 1 Reed-Maldonado AB, Madden KC. Infertility and the Military Male. *Semin Reprod Med*, 2019,37(1):5-11
- 2 Nagata MPB, Endo K, Ogata K, *et al.* Live births from artificial insemination of microfluidic-sorted bovine spermatozoa characterized by trajectories correlated with fertility. *Proc Natl Acad Sci USA*, 2018,115(14):E3087-E3096
- 3 Holka-Pokorska J, Jarema M, Wichniak A. Clinical determinants of mental disorders occurring during the infertility treatment. *Psychiatr Pol*, 2015,49(5):965-982
- 4 Punab M, Poolamets O, Paju P, *et al.* Causes of male infertility: a 9-year prospective monocentre study on 1737 patients with reduced total sperm counts. *Hum Reprod*, 2017,32(1):18-31
- 5 Chen X, Ma Y, Zou S, *et al.* Comparison and outcomes of nonobstructive azoospermia patients with different etiology undergoing MicroTESE and ICSI treatments. *Transl Androl Urol*, 2019,8(4):366-373
- 6 Corona G, Minhas S, Giwercman A, *et al.* Sperm recovery and ICSI outcomes in men with non-obstructive azoospermia: a systematic review and meta-analysis. *Hum Reprod Update*, 2019,25(6):733-757
- 7 Zhao P, Gu X, Wu H, *et al.* Molecular and cytogenetic analysis of infertile Hakka men with azoospermia and severe oligozoospermia in southern China. *J Int Med Res*, 2019,47(3):1114-1123
- 8 Coutton C, Fissore RA, Palermo GD, *et al.* Male Infertility: Genetics, Mechanism, and Therapies. *Biomed Res Int*, 2016,2016:7372362
- 9 Xavier MJ, Salas-Huetos A, Oud MS, *et al.* Disease gene discovery in male infertility: past, present and future. *Hum Genet*, 2021,140(1):7-19
- 10 Ferlin A, Raicu F, Gatta V, *et al.* Male infertility: role of genetic background. *Reprod Biomed Online*, 2007,14(6):734-745
- 11 N DF, Amir A-Y, Guillaume M, *et al.* Absence of CFAP69 Causes Male Infertility due to Multiple Morphological Abnormalities of the Flagella in Human and Mouse. *Am J Hum Genet*, 2018,102(4):636-648
- 12 Tanaka H, Iguchi N, Toyama Y, *et al.* Mice deficient in the axonemal protein Tektin-t exhibit male infertility and immotile-cilium syndrome due to impaired inner arm dynein function. *Mol Cell Biol*, 2004,24(18):7958-7964
- 13 Kuo YC, Lin YH, Chen HI, *et al.* SEPT12 mutations cause male infertility with defective sperm annulus. *Hum Mutat*, 2012,33(4):710-719
- 14 Aminata T, Pierre L, A GJ, *et al.* The testis anion transporter 1 (Slc26a8) is required for sperm terminal differentiation and male fertility in the mouse. *Hum Mol Genet*, 2007,16(15):1783-1793
- 15 Auguste Y, Delague V, Desvignes JP, *et al.* Loss of Calmodulin- and Radial-Spoke-Associated Complex Protein CFAP251 Leads to Immotile Spermatozoa Lacking Mitochondria and Infertility in Men. *Am J Hum Genet*, 2018,103(3):413-420
- 16 Zhou Y, Li K, Du Y, *et al.* Protein interacting with C-kinase 1 is involved in epithelial-mesenchymal transformation and suppresses progress of gastric cancer. *Med Oncol*, 2021,38(34):1-11
- 17 Xiao N, Kam C, Shen C, *et al.* PICK1 deficiency causes male infertility in mice by disrupting acrosome formation. *J Clin Invest*, 2009,119(4):802-812
- 18 Liu G, Shi QW, Lu GX. A newly discovered mutation in PICK1 in a human with globozoospermia. *Asian J Androl*, 2010,12(4):556-560
- 19 de Lamirande E. Semenogelin, the main protein of the human semen coagulum, regulates sperm function. *Semin Thromb Hemost*, 2007,33(1):60-68
- 20 Lwaleed BA, Greenfield R, Stewart A, *et al.* Seminal clotting and fibrinolytic balance: a possible physiological role in the male reproductive system. *Thromb Haemost*, 2004,92(4):752-766
- 21 Hanley JG. PICK1: A multi-talented modulator of AMPA receptor trafficking. *Pharmacology & Therapeutics*, 2008,118(1):152-160
- 22 Kamano Y, Watanabe J, Iida T, *et al.* Binding of PICK1 PDZ domain with calcineurin B regulates osteoclast differentiation. *Biochem Biophys Res Commun*, 2018,496(1):83-88
- 23 Cao M, Xu J, Shen C, *et al.* PICK1-ICA69 heteromeric BAR domain complex regulates synaptic targeting and surface expression of AMPA receptors. *J Neurosci*, 2007,27(47):12945-12956
- 24 He J, Xia M, Tsang WH, *et al.* ICA1L forms BAR-domain complexes with PICK1 and is crucial for acrosome formation in spermiogenesis. *J Cell Sci*, 2015,128(20):3822-3836
- 25 Yang Z, Gallicano GI, Yu QC, *et al.* An unexpected localization of basenuclin in the centrosome, mitochondria, and acrosome of developing spermatids. *J Cell Biol*, 1997,137(3):657-669
- 26 Hossain MS, Johannisson A, Wallgren M, *et al.* Flow cytometry for the assessment of animal sperm integrity and functionality: state of the art. *Asian J Androl*, 2011,13(3):406-419
- 27 Li Y, Li C, Lin S, *et al.* A nonsense mutation in Ccdc62 gene is responsible for spermiogenesis defects and male infertility in repro29/repro29 mice. *Biol Reprod*, 2017,96(3):587-597
- 28 Hirawatari K, Hanzawa N, Miura I, *et al.* A Cascade of epistatic interactions regulating teratozoospermia in mice. *Mamm Genome*, 2015,26(5-6):248-256
- 29 Saraf KK, Kumaresan A, Chhillar S, *et al.* Spermatozoa with high mitochondrial membrane potential and low tyrosine phosphorylation preferentially bind to oviduct explants in the water buffalo (*Bubalus bubalis*). *Anim Reprod Sci*, 2017,180:30-36
- 30 Lwaleed BA, Goyal A, Delves GH, *et al.* Seminal hemostatic factors: then and now. *Semin Thromb Hemost*, 2007,33(1):3-12
- 31 Wang YW, Du YQ, Miao XL, *et al.* Risk factors and drug resistance in early-onset neonatal group B streptococcal disease. *J Zhejiang Univ-SCIE B*, 2018,19(12):973-978
- 32 Jiao SY, Yang YH, Chen SR. Molecular genetics of infertility: loss-of-function mutations in humans and corresponding knockout/mutated mice. *Hum Reprod Update*, 2021,27(1):154-189
- 33 Du Y, Li Z, Liu Z, *et al.* Nonrandom occurrence of multiple de novo coding variants in a proband indicates the existence of an oligogenic model in autism. *Genet Med*, 2020,22(1):170-180
- 34 Du Y, Wang H, Chen L, *et al.* Non-RBM Mutations

- Impaired SARS-CoV-2 Spike Protein Regulated to the ACE2 Receptor Based on Molecular Dynamic Simulation. *Front Mol Biosci*, 2021,8:614443
- 35 Jiang X, Zhang H, Yin S, *et al.* Specific deficiency of Plzf paralog, Zbtb20, in Sertoli cells does not affect spermatogenesis and fertility in mice. *Sci Rep*, 2014,4:7062
- 36 DamAH, FeenstraI, WestphalJR, *et al.* Globozoospermia revisited. *Hum Reprod Update*, 2007,13(1):63-75
- 37 Zhang R, Niu G, Li X, *et al.* Reaction-free and MMP-independent fluorescent probes for long-term mitochondria visualization and tracking. *Chem Sci*, 2019,10(7):1994-2000
- 38 Schneider S, Shakeri F, Trotschel C, *et al.* Protamine-2 Deficiency Initiates a Reactive Oxygen Species (ROS)-Mediated Destruction Cascade during Epididymal Sperm Maturation in Mice. *Cells*, 2020,9(8):1789
- 39 Xie D, Lu C, Zhu Y, *et al.* Analysis on the association between sperm DNA fragmentation index and conventional semen parameters, blood microelements and seminal plasma ROS in male patients with infertility. *Exp Ther Med*, 2018,15(6):5173-5176
- 40 Liu CH, Tsao HM, Cheng TC, *et al.* DNA fragmentation, mitochondrial dysfunction and chromosomal aneuploidy in the spermatozoa of oligoasthenoteratozoospermic males. *J Assist Reprod Genet*, 2004,21(4):119-126
- 41 Ambulkar PS, Chuadhari AR, Pal AK. Association of large scale 4977-bp "common" deletions in sperm mitochondrial DNA with asthenozoospermia and oligoasthenoteratozoospermia. *J Hum Reprod Sci*, 2016,9(1):35-40
- (Received Mar. 20, 2022; accepted Sep. 2, 2022)